

Temperature Modulated Calorimetry of Glassy Polymers and Polymer Blends

E. Flikkema, G. Alberda van Ekenstein, and G. ten Brinke*

Laboratory of Polymer Chemistry, Materials Science Center, University of Groningen, Nijenborgh 4, 9747 AG Groningen, The Netherlands

Received June 20, 1997; Revised Manuscript Received November 24, 1997

ABSTRACT: The theoretical modeling of the relaxation behavior of polymers in the glass transition region, advocated by Moynihan and co-workers, has been used to analyze the heat flow and the relaxation of polymer systems during isothermal modulated DSC experiments in the glass transition region. An analytic solution for the frequency dependent fictive temperature is obtained, which takes a particularly simple form in the high-frequency region. The maximal phase lag of the fictive temperature T_f is $\beta\pi/2$, where the exponent of the stretched-exponential characterizing the enthalpy relaxation, β , is on the order of 0.1–0.7. The corresponding maximal phase lag in the heat flow is much smaller, on the order of 2–5 deg. It is once more iterated that, as observed long ago by Birge and Nagel, the loss heat capacity corresponds to the entropy production due to a redistribution of energy over the heat baths. The possibility of using specific-heat spectroscopy as a tool to determine miscibility in polymer blends whose constituents possess similar glass transition temperatures is discussed. Compared to conventional differential scanning calorimetry, the resolution is enhanced. However, in many cases an unambiguous conclusion still requires additional enthalpy relaxation of the blend induced by physical aging in the glassy state.

1. Introduction

Steady-state ac calorimetry was introduced more than 30 years ago as a method for measuring heat capacity.¹ Specific heat spectroscopy, measuring the frequency dependent specific heat from the response of a sample to a sinusoidal temperature profile, is of a more recent date.^{2–7} In a pioneering paper, Birge and Nagel² discussed its application to the glass transition of glycerol. They also clarified the precise thermodynamic relation between the presence of a complex heat capacity and entropy production. The adaptation of conventional DSC to include these possibilities occurred only recently. It was commercialized some time ago under the name of Modulated DSC.⁸ Various groups have been heavily involved in the further development of this new method, notably the groups around Reading,^{9–11} Schawe,^{12–14} and Wunderlich^{15–18} but also others.¹⁹

With the advent of temperature-modulated DSC, there is an increased interest in the theoretical description of the response of a polymer system to a temperature-modulated profile. This is particularly true for the glass transition region where phase lag phenomena are prominently present. The most simple experiment consists of subjecting the sample to a small-amplitude temperature-modulated profile under otherwise isothermal conditions. Far above the glass transition temperature, the system will remain in equilibrium at all times. Considerably below the glass transition temperature, on the other hand, the system will not respond structurally to the changing temperature. In both cases the heat flow will be in phase with the temperature modulation. When the temperature is decreased from above the glass transition temperature through the transition region, the structural relaxations will gradually diminish. These relaxations are usually discussed in terms of the fictive temperature, T_f , defined as the temperature at which the structure would be at equilibrium.

At temperatures sufficiently far above the glass transition temperature T_f will be identical to the temperature and thus follow the modulated profile. Somewhat below the glass transition temperature, T_f will be equal to the isothermal starting conditions, independent of the modulation. In the glass transition region, T_f will exhibit the same modulated behavior as the imposed temperature modulation. However, it will do so with a smaller amplitude and with a phase lag.

In the following sections we will briefly summarize the description of the relaxation behavior of polymer systems as introduced by Moynihan and co-workers.²⁰ We will demonstrate its consequences with respect to the response of the fictive temperature T_f to a modulated temperature profile and discuss the consequences for the experimentally observed heat flow. The procedure resembles the recently published description by Hutchinson and Montserrat¹⁹ using a single relaxation time model and is effectively the counterpart of the Kovacs and co-workers multiorder parameter theory (KAHR).²¹ One advantage of our approach is that it leads to closed expressions for the quantities involved that are rather transparent. In this way, a very simple picture emerges. We will also consider briefly the connection between the imaginary part of the specific heat capacity, where we follow Birge and Nagel² in demonstrating via very simple thermodynamic arguments how it is precisely related to the entropy production in the heat baths. Finally we will discuss the application of specific-heat spectroscopy to polymer blends. The emphasis will be on blends whose constituents have similar glass transition temperatures.

2. Model

For a given temperature trajectory $T(t)$, as a function of time t , the fictive temperature $T_f(t)$ can, according to the theoretical approach introduced by Moynihan and

co-workers,²⁰ be calculated by the expression

$$T_f(t) = T_0 + \int_0^t dt' \frac{dT(t')}{dt'} \left\{ 1 - \exp \left[- \left(\int_{t'}^t \frac{dt''}{\tau(T(t''), T_f(t''))} \right)^\beta \right] \right\} \quad (1)$$

where the mean relaxation time τ obeys the empirical form first suggested by Narayanaswamy²²

$$\tau(T, T_f) = A \exp \left[\frac{x\Delta h}{RT} + \frac{(1-x)\Delta h}{RT_f} \right] \quad (2)$$

Here A , x , and Δh are phenomenological constants. x has a value between 0 and 1 and is called the nonlinearity parameter; Δh governs the rate at which the fictive temperature changes with the rate of cooling,^{22,23} and β is the exponent of the stretched-exponential describing the relaxation of the enthalpy H .

This description of the relaxation behavior of glassy polymers is known to suffer from several shortcomings.²⁴ However, since it is also known to describe most of the experimental enthalpy relaxation data quite well,^{25–28} it is expected to describe the response to an isothermal temperature-modulated profile at least equally well.

In the past, eq 1 has been used frequently as a starting point to calculate numerically the normalized specific heat during a conventional DSC scan, including aging.^{23,25–28} This is realized by discretizing the integrals:

$$T_f[n] = T[0] + \sum_{j=1}^n (T[j] - T[j-1]) \left\{ 1 - \exp \left[- \left(\sum_{k=j}^n \frac{t[k] - t[k-1]}{\tau(T[k], T_f[k-1])} \right)^\beta \right] \right\} \quad (3)$$

$T[k]$ is the value of T at time $t[k]$. The recurrence relation allows us to calculate $T_f[n]$ from $T[0]$, ..., $T[n]$, $t[0]$, ..., $t[n]$ and $T_f[0]$, ..., $T_f[n-1]$. Computation time is reduced if one stores the values of the inner sum (for each j) in an array:

$$s[j] = \sum_{k=j}^n \frac{t[k] - t[k-1]}{\tau(T[k], T_f[k-1])} \quad (4)$$

Going from $n-1$ to n , one needs to update $s[j]$ in the following way:

$$t = \frac{t[n] - t[n-1]}{\tau(T[n], T_f[n-1])} \quad (5)$$

$$s[j] = s[j] + t \quad \text{for } j = 1, \dots, n-1 \quad (6)$$

$$s[n] = t \quad (7)$$

The normalized specific heat $C_p^N(t)$ is related to $T_f[n]$ by

$$C_p^N(t[n]) \equiv \frac{C_p(t[n]) - C_{pg}}{C_{pl} - C_{pg}} = \frac{T_f[n] - T_f[n-1]}{T[n] - T[n-1]} \quad (8)$$

where C_{pl} and C_{pg} are the heat capacities in the liquid and glassy states, respectively. The heat flow corresponding to a temperature trajectory $T(t)$ is related to

$T_f(t)$ by

$$\frac{dQ}{dt} = C_{pg} \frac{dT}{dt} + (C_{pl} - C_{pg}) \frac{dT_f}{dt} \quad (9)$$

The first issue we are going to address is the response of T_f to a sinusoidal input $T(t)$:

$$T(t) = T_0 + a \sin(\omega t) \quad (10)$$

which corresponds to an isothermal modulated DSC experiment. After some time $T_f(t)$ settles to a sinusoidal form as well:

$$T_f(t) = T_0 + a' \sin(\omega t - \varphi) \quad (11)$$

Our main interest here is the frequency dependence of the amplitude a' and the phase lag φ . Now, any linear and time-invariant system has the following property: if the system is subjected to a sinusoidal stimulus the output will also be sinusoidal with the same frequency, though generally with a different amplitude and a shifted phase. The transfer-function $\hat{f}(\omega)$ is a complex-valued function: the absolute value $|\hat{f}(\omega)|$ corresponds to the ratio of the amplitude of the output signal and the amplitude of the incoming signal. The argument $\arg(\hat{f}(\omega))$ corresponds to the phase shift of the output signal with respect to the incoming signal. Our aim is to compute the transfer-function $f(\omega)$ when $T(t)$ is the incoming signal and $T_f(t)$ is the output signal. To this end we start from Eqs 1–2. We will consider a very small modulation amplitude. In that case eq 1 may be linearized by replacing $\tau^{-1}(T(t'), T_f(t'))$ by the constant

$$\tau^{-1}(T(t'), T_f(t')) \cong \tau^{-1}(T_0, T_0) = A^{-1} \exp \left[- \frac{\Delta h}{RT_0} \right] \quad (12)$$

We denote the right-hand side of eq 12 by c . So, we have

$$\int_{t'}^t dt'' \tau^{-1}(T(t''), T_f(t'')) \cong \int_{t'}^t dt'' \tau^{-1}(T_0, T_0) = c(t - t') \quad (13)$$

The linearized expression for T_f is

$$T_f(t) - T_0 \cong \int_0^t dt' \frac{dT(t')}{dt'} \{ 1 - \exp[-c(t - t')]^\beta \} \quad (14)$$

This is a convolution of $dT(t)/dt$ and $g(t)$ where

$$g(t) = 1 - \exp[-(ct)^\beta] \quad \text{if } t > 0$$

$$g(t) = 0 \quad \text{if } t \leq 0 \quad (15)$$

The fact that $g(t) = 0$ for $t \leq 0$ expresses the principle of causality. By defining $\Delta T(t) \equiv T(t) - T_0$ and $\Delta T_f(t) \equiv T_f(t) - T_0$ and performing a partial integration we obtain

$$\Delta T_f(t) = \int_0^t dt' \Delta T(t') f(t - t') \quad (16)$$

with

$$f(t) = g'(t) = \beta c^\beta t^{\beta-1} \exp[-(ct)^\beta] \quad (17)$$

Hence

$$\Delta \hat{T}_f(\omega) = \hat{H}(\omega) \Delta \hat{T}(\omega) \quad (18)$$

where

$$\hat{H}(\omega) = \beta c^\beta \int_0^\infty dt t^{\beta-1} e^{-(ct)^\beta} e^{-i\omega t} \quad (19)$$

This integral can be solved by using the Taylor expansion for $e^{-(ct)^\beta}$

$$\begin{aligned} \hat{H}(\omega) &= \beta c^\beta \sum_{k=0}^{\infty} \frac{(-1)^k}{k!} \int_0^\infty dt (ct)^{k\beta} t^{\beta-1} e^{-i\omega t} = \\ &= \sum_{k=1}^{\infty} \left(\frac{c}{\omega} \right)^{k\beta} \frac{(-1)^{k-1}}{k!} \Gamma(k\beta + 1) e^{-i\pi k\beta/2} \quad (20) \end{aligned}$$

where Γ denotes the gamma function. In the “high”-frequency limit this implies

$$\hat{H}(\omega) = \left(\frac{c}{\omega} \right)^\beta \Gamma(\beta + 1) e^{-i\pi\beta/2} \quad (21)$$

In this case the amplitude ratio and the phase lag are very simple:

$$\frac{a'}{a} = \left(\frac{c}{\omega} \right)^\beta \Gamma(\beta + 1) \quad \text{and} \quad \varphi = \frac{\pi\beta}{2} \quad (22)$$

Note that in this limit the phase lag of the fictive temperature only depends on the width of the relaxation spectrum, i.e., β . Since the amplitude depends on the other parameters involved through c , the phase lag of the heat flow (eq 9) will obviously depend on all parameters.

Applications

Although the frequency-dependent specific heat for simple glass-forming liquids has already been measured over a wide frequency range (4 mHz to 8 kHz),⁷ for the commercial modulated DSC equipment the period of the modulation is on the order of 30–600 s. Whether this is in the high-frequency regime will depend on the temperature. To investigate this, the full expression in eq 1 has been used to calculate the amplitude ratio and the phase lag as a function of frequency for a polymer system which within the Moynihan description has the parameter values used before for polystyrene²⁸ and presented in Table 1. Furthermore, we take $T_0 = 375$ K and a very small modulation amplitude, $a = 0.01$ K, the latter only to ensure the strict validity of the linearization of eq 12. Figures 1 and 2 present the numerical data obtained by the full calculations for the amplitude ratio and the phase lag, respectively. In Figure 1, the high-frequency result in eq 22 is also indicated, demonstrating that the agreement is excellent up to rather low frequencies. The same holds true for the phase lag, where we notice that it approaches the limiting high-frequency value also already at rather low frequencies. At this particular temperature, the modulated periods of 30–600 s are clearly inside the limiting regime. In this range the phase lag of T_f will be considerable, on the order of $\pi/4$, and the amplitude ratio will still be on the order of 0.2. However, the structural relaxations, manifested in the behavior of T_f , are only a small part of the heat flow, and this will now be addressed in more detail.

Equations 9–11 imply that the total heat flow is given by

Table 1. Narayanaswamy Parameters

polymer	β	$\ln A$	x	$10^{-3}\Delta h/R$ (K)	C_{pg} (J/gK) ^d	C_{pl} (J/gK) ^d
PS ^a	0.47	−329	0.24	126	1.368	1.730
PMMA ^b	0.35	−358	0.19	138	1.448	1.898
PVC ^c	0.25	−619	0.11	225	1.119	1.431

^a Reference 28. ^b Reference 23. ^c Reference 26. ^d Specific heat data measured by author (G. A.).

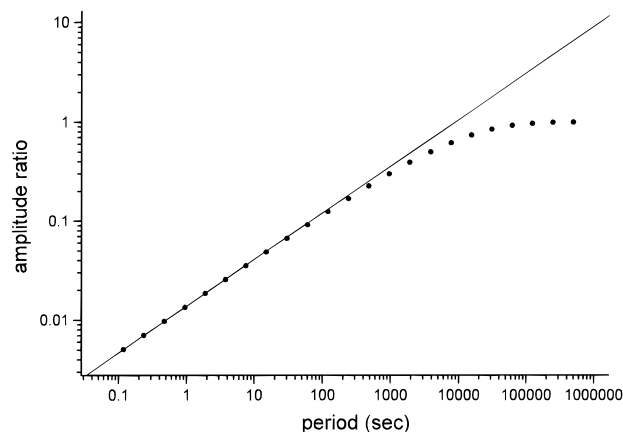


Figure 1. Amplitude ratio between the amplitude a' of T_f and the amplitude of the temperature modulation $a = 0.01$ K as a function of the period, for $T_0 = 375$ K, and parameter values of PS presented in Table 1. Points represent full calculation; solid line represents the high-frequency limit (eq 22).

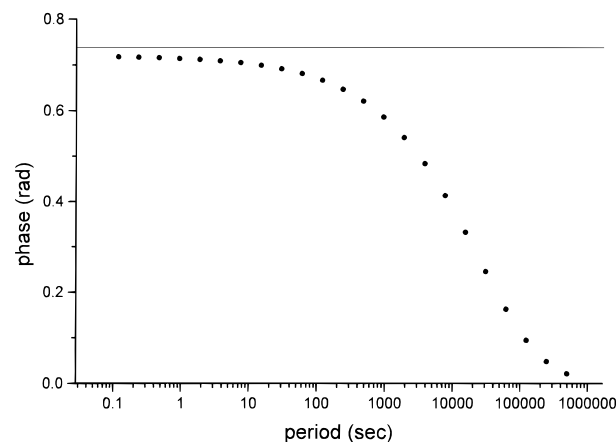


Figure 2. Phase lag of T_f as a function of the period for a temperature modulation with amplitude $a = 0.01$ K, $T_0 = 375$ K, and parameter values of PS presented in Table 1. Points represent full calculation; solid line represents high-frequency limit (eq 22).

$$\begin{aligned} \frac{dQ}{dt} &= a\omega C_{pg} \cos(\omega t) + a'\omega (C_{pl} - C_{pg}) \cos(\omega t - \varphi) = \\ &= a'\omega \cos(\omega t - \varphi') \quad (23) \end{aligned}$$

where the amplitude a' and the phase lag φ' are the parameters of interest. They follow straightforwardly, by simple trigonometric arguments from this relation together with the input of a'/a and φ . For the high-frequency limit these were explicitly given by eq 22; in all other cases, numerical results such as those presented in Figures 1 and 2 have to be used. Equation 23 can also be written in the form

$$\frac{dQ}{dt} = a\omega [C_p(\omega) \cos(\omega t) + C'_p(\omega) \sin(\omega t)] \quad (24)$$

where the frequency-dependent complex specific heat

is given by¹²

$$C_p(\omega) = C_p(\omega) + iC'_p(\omega) \quad (25)$$

Before we continue with the numerical calculation of the phase lag, it is worthwhile to consider briefly the thermodynamic implication of the presence of a complex heat capacity. Although noted by various authors lately,^{13,17,19} Birge and Nagel² pointed out already many years ago that the usual implication of an imaginary part of a linear susceptibility of a net absorption of energy by the sample from the applied field (cf. dynamic mechanical spectroscopy) does not hold here. Nevertheless, it does signify the presence of entropy production. During a full cycle, the system returns back to its original state and so does its entropy. This, however, is not the case for the "heat bath". From a thermodynamic viewpoint, the minimal entropy change of the "heat bath" is given by

$$\Delta S = - \int_{t=0}^{t=2\pi/\omega} \frac{dQ_{rev}}{T} \quad (26)$$

where dQ_{rev} is the heat reversibly transferred from the heat bath to the system. Since this process has to take place reversibly, we actually have to imagine the presence of an infinite series of heat baths, one corresponding to every temperature. As long as the imaginary part of the specific heat of the system is 0, the amount of heat transferred from a particular heat bath to the system during the heating part of the cycle is exactly returned to the same heat bath during the cooling part of the cycle. The maximum amount of heat for instance, is absorbed by the system at T_0 during heating and returned during cooling. However, this is no longer the case for $C'_p > 0$. Now the system absorbs the maximum amount of heat at a temperature above T_0 and returns this amount at a temperature below T_0 . Similar observations are valid for the complete cycle and consequently, this redistribution of energy between the heat baths leads to an increase of entropy by the heat baths given by

$$\Delta S = - \int_0^{2\pi/\omega} \frac{1}{T(t)} \frac{dQ(t)}{dt} dt = \pi C'_p(\omega) \left(\frac{a}{T_0} \right)^2 \quad (27)$$

The right-hand side follows from eqs 10 and 25 using $a/T_0 \ll 1$. As is clear, the second law of thermodynamics actually requires $C'_p \geq 0$, or alternatively that $\varphi' \geq 0$.

A full calculation of the phase lag φ' for the parameter values of PS listed in Table 1, for different values of the temperature, is presented in Figure 3. The figures clearly resemble the familiar $\tan \delta$ plots for dynamic mechanical spectroscopy (DMS). Since the phase lag is rather small, ≤ 0.055 rad, a plot of $\tan \varphi'$ is obviously almost identical. The maximum value of the phase lag of the heat flow amounts to only 10% of the high-frequency phase lag of the fictive temperature (Figure 2). This was to be expected, since eq 9 clearly shows that the structural relaxation contribution, giving rise to the phase lag, is only a small part of the total heat flow. Figure 3 demonstrates that the theoretical model predicts a near constancy in the peak amplitude and the shape of the loss curves as a function of temperature. This so-called time-temperature superposition principle is a consequence of the model. However, there is a growing body of evidence^{6,7} showing that the

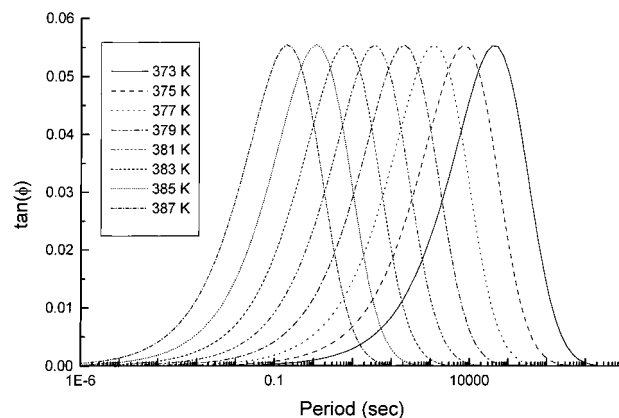


Figure 3. Phase lag of the heat flow for a series of temperatures as a function of the period for a temperature modulation with amplitude $a = 0.5$ K and parameter values of PS presented in Table 1.

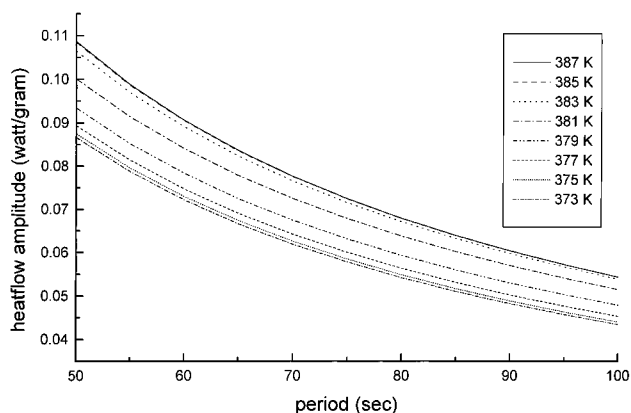


Figure 4. Heat flow amplitude as a function of the period, for a series of temperatures corresponding to a temperature modulation with amplitude $a = 0.5$ K. Parameter values are those of PS listed in Table 1.

William-Watts fitting parameter β is a function of temperature. In many cases the relaxation peaks broaden as the temperature is lowered implying a decreasing value of β . Hence, when used, the time-temperature superposition procedure should be restricted to a narrow temperature range. Figure 4, finally presents the heat flow amplitude $(a'/a)\omega$ as a function of the period for various temperatures in the experimentally accessible range.

DSC is often the preferred technique to investigate miscibility in polymer blends, a composition dependent glass transition temperature being indicative of homogeneous mixing. This simple criterion obviously fails for blends whose constituents possess similar glass transition temperatures. Several years ago we demonstrated that the phenomenon of enthalpy relaxation in the amorphous glassy state can be employed as an alternative thermal analysis procedure.^{29,30} Here the appearance of multiple or asymmetric enthalpy recovery peaks during heating through the glass transition region is taken as conclusive evidence for heterogeneous mixing. Conversely, a single sharp recovery peak is characteristic for homogeneous mixtures. The basis of this technique is essentially the fact that the enthalpy relaxation procedure probes many more details of the relaxation spectrum than a simple T_g measurement. These details are different for different polymers, even though their glass transition temperatures are approximately the same. Since modulated DSC also

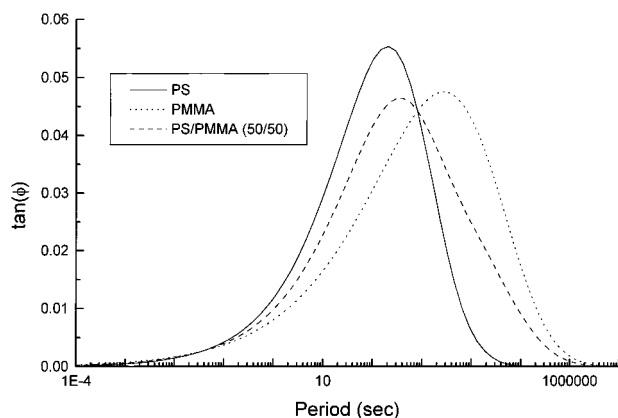


Figure 5. Phase lag $\tan \phi'$ for pure PS, pure PMMA, and an immiscible 50/50 wt % PS/PMMA blend, calculated on the basis of the parameter values presented in Table 1, as a function of the period for $T = 379$ K.

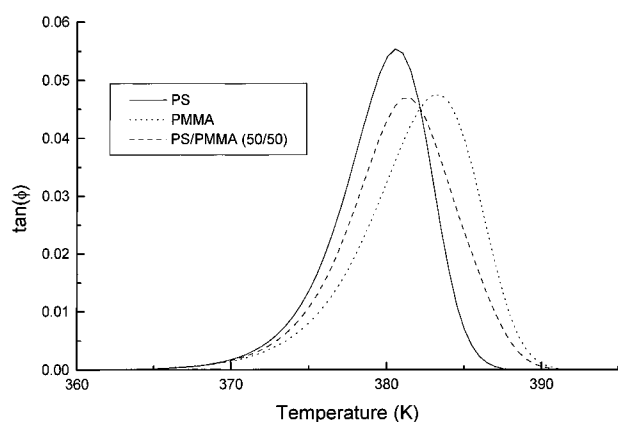


Figure 6. Phase lag $\tan \phi'$ for pure PS, pure PMMA, and an immiscible 50/50 wt % PS/PMMA blend, calculated on the basis of the parameter values presented in Table 1, as a function of temperature for a fixed period of 50 s.

probes the relaxation spectrum rather than an average property, this suggests that specific-heat spectroscopy may be used as an alternative technique to determine (im)miscibility for this class of blends. To investigate this we compared the calculated $\tan \phi'$ as a function of temperature and frequency for different sets of parameter values. For the first pair we took polystyrene (PS) and poly(methyl methacrylate) (PMMA), for which the parameter values are listed in Table 1. Both sets of parameters correspond to a T_g (onset) of approximately 100 °C. Figure 5 shows $\tan \phi'$ as a function of frequency, at $T = 379$ K, for pure PS, PMMA, and a 50/50 wt % blend, the latter obtained by simple additivity motivated by the known immiscibility. The positions, heights, and widths of the peaks for the pure polymers differ slightly. As a consequence, the immiscibility of the blend becomes visible as an extremely small low frequency shoulder only. Figure 6 shows $\tan \phi'$ for the same systems, now as a function of temperature for the characteristic frequency corresponding to a period of 50 s. The results are very similar to those just presented. Hence, for this particular case, even very accurate measurements will not be able to determine the phase behavior. As for conventional DSC, modulated DSC also is incapable of determining miscibility between components with very similar T_g values. If polymers with a somewhat larger difference in T_g values are selected, two peaks will appear in the blend in case of immiscibility. To illustrate this, besides PS

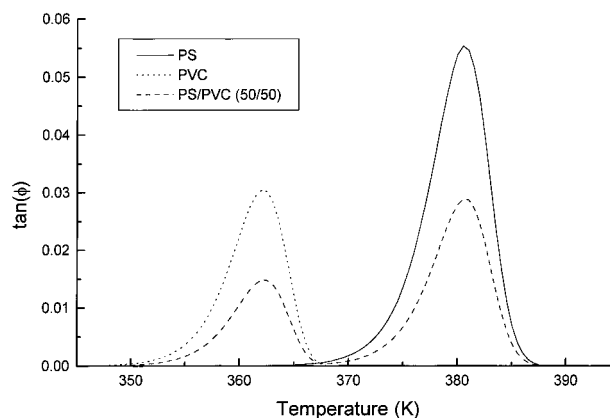


Figure 7. Phase lag $\tan \phi'$ for pure PS, pure PVC, and an immiscible 50/50 wt % PS/PVC blend, calculated on the basis of the parameter values listed in Table 1, as a function of temperature for a fixed period of 50 s.

poly(vinyl chloride) (PVC) with a T_g of approximately 85 °C was chosen as the second component. Table 1 contains the relevant (parameter) values for PVC. For PVC as well as PMMA, the very small values of x have been questioned recently,³¹ however, for illustrative purposes the precise values are rather unimportant, the difference in T_g values is what matters. Figure 7 shows $\tan \phi'$ for PS, PVC, and a 50/50 wt % blend as a function of temperature. Assuming again complete immiscibility, it is observed that the blend is now characterized by two clearly separated peaks. From these two examples and similar calculations involving PS and hypothetical polymers with T_g values between those of PMMA and PVC, it follows that the $\tan \phi'$ vs temperature curves of polymers with similar glass transition temperatures will be sufficiently different to let immiscibility show up if the difference in T_g value is on the order of 5 °C. If the relaxation spectrum of the two polymers is very different, i.e., a large difference in β values, immiscibility may show up in the form of a shoulder for T_g values that are even closer than 5 °C. Hence, modulated DSC will ultimately be able to resolve miscibility in polymer blends containing components with glass transition temperatures which are less different than necessary for conventional DSC, where the single/double T_g criterion requires the T_g 's to differ by ca. 10 K.

Still, for many cases the enthalpy relaxation procedure will remain the only thermal analysis technique available to reach a definite conclusion. However, despite this observation, even in this case the use of temperature-modulated DSC in combination with enthalpy relaxation provides additional information not available from conventional DSC. As a simple concrete example of what is possible at this moment with the commercially available instrumentation, Figures 8–11 present the experimental data for a 50/50 wt % blend of PS ($T_g = 104.3$ °C) and a random copolymer of styrene and *p*-fluorostyrene (P(S-*p*FS67), 67 mol % *p*FS, $T_g = 108.3$ °C). Figure 8 presents the total heat flow for samples which have been annealed for the indicated amounts of time in the glassy state at 92 °C. The fact that both components are immiscible, as reported before,³² is obvious from the enthalpy recovery peak(s), but only after annealing for more than 46 h. Without annealing, a single glass transition is observed. These measurements have been analyzed by the semiempirical procedure introduced by Reading.¹⁰ In this procedure,

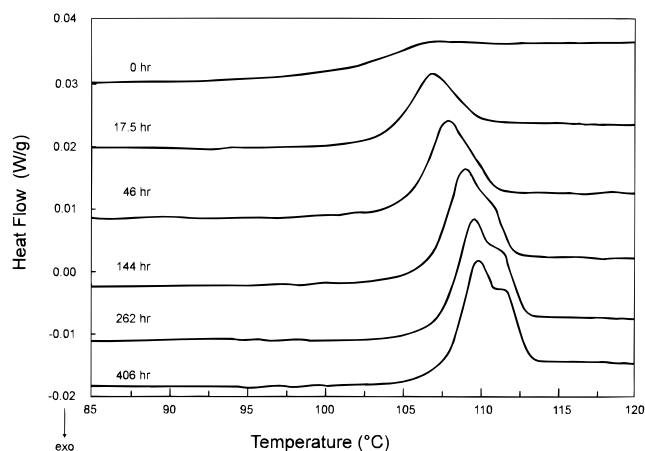


Figure 8. Total heat flow for 50/50 wt % blends of PS and P(S-pFS67) annealed at 92 °C, for the indicated amounts of time.

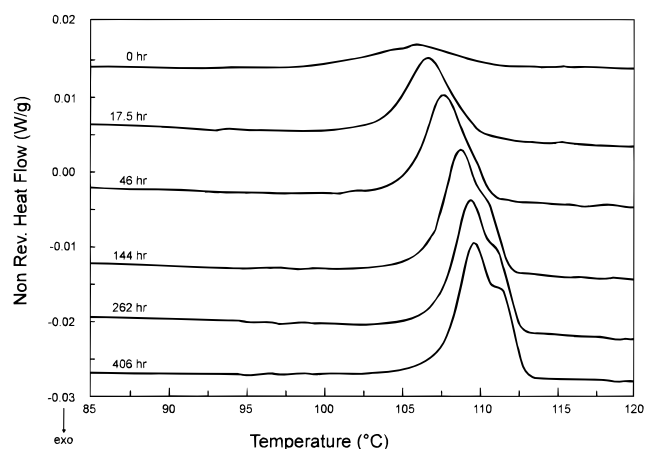


Figure 9. Nonreversing heat flow curves of PS/P(S-pFS67) (50/50 wt %) annealed at 92 °C, for the indicated amounts of time.

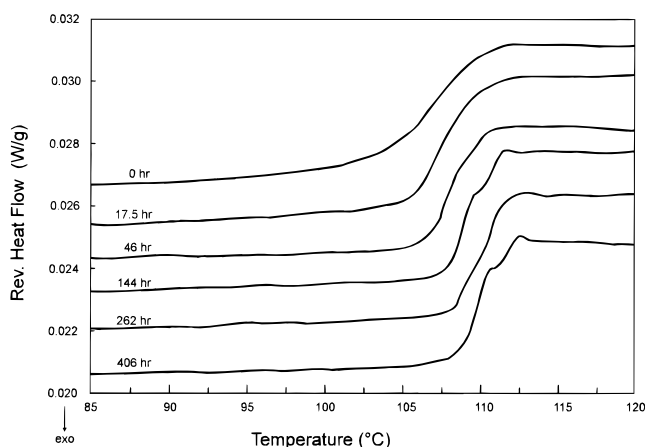


Figure 10. Reversing heat flow curves of PS/P(S-pFS67) (50/50 wt %) annealed at 92 °C, for the indicated amounts of time.

the heat flow is separated in a reversing and a nonreversing component, the latter being the difference between the total heat flow and the reversing heat flow. Enthalpy recovery is clearly a nonreversing process, and Figure 9, presenting the nonreversing heat flow, confirms this. Again the development of two separate peaks is obvious. The occurrence of a small peak in the unannealed samples is a manifestation of the relaxation processes going on during the scan. Figure 10 presents the reversing component and shows that the inhomogeneous nature of the system does manifest itself also here, but again, only after annealing. Once the sample is annealed for a long period of time, the glass transition temperatures are sufficiently different to show up. The derivative of the reversing heat flow is presented in the last figure; from its peak temperatures the separate T_g 's (deflection) can be determined, something that is impossible by conventional DSC.

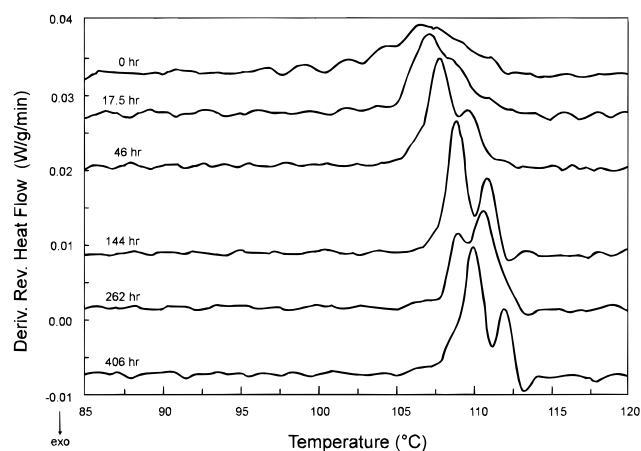


Figure 11. Derivative reversing heat flow corresponding to the data in Figure 10.

geneous nature of the system does manifest itself also here, but again, only after annealing. Once the sample is annealed for a long period of time, the glass transition temperatures are sufficiently different to show up. The derivative of the reversing heat flow is presented in the last figure; from its peak temperatures the separate T_g 's (deflection) can be determined, something that is impossible by conventional DSC.

Concluding Remarks

In the previous sections we discussed specific-heat spectroscopy in the framework of the Moynihan et al.²⁰ approach. Although the technique itself is already quite old, its large scale application to polymer systems is of a very recent date. One of the obvious advantages of temperature-modulated DSC is the possibility to separate overlapping signals when a glass transition and exothermic processes are present.³³⁻³⁵ Our results demonstrate that it also is of a more fundamental interest, since the parameters of the theoretical description of the relaxation behavior of polymers in the glassy state (notably β and $A^{-1} \exp[\Delta h/RT]$ in the case considered here) can in principle be obtained once accurate experimental data are available.

Furthermore, it was demonstrated that modulated DSC provides more detailed information about the relaxation processes in the glass transition region, which implies that the resolution of this technique regarding (im)miscibility of polymers with similar glass transition temperatures is enhanced compared to conventional DSC. Still, in many cases, the enthalpy relaxation procedure introduced several years ago remains the only thermal analysis technique to determine miscibility in polymer blends. Nevertheless, also here this new technique provides additional information which is particularly useful in those cases where additional complications due to endothermic/exothermic processes occur.³³⁻³⁵

References and Notes

- (1) Sullivan, P. F.; Seidel, G. *Phys. Rev.* **1968**, *173*, 679.
- (2) Birge, N. O.; Nagel, S. R. *Phys. Rev. Lett.* **1985**, *54*, 2674.
- (3) Oxtoby, D. W. *J. Chem. Phys.* **1986**, *85*, 1549.
- (4) Zwanig, R. J. *Chem. Phys.* **1988**, *88*, 5831.
- (5) Dixon, P. K. *Phys. Rev.* **1990**, *B 42*, 8179.
- (6) Dixon, P. K.; Nagel, S. R. *Phys. Rev. Lett.* **1988**, *61*, 341.
- (7) Menon, N. J. *Chem. Phys.* **1996**, *105*, 5246.
- (8) Gill, P. S.; Sauerbrunn, S. R.; Reading, M. J. *Therm. Anal.* **1993**, *40*, 931.
- (9) Reading, M. *Trends Polym. Sci.* **1993**, *1*, 248.

- (10) Reading, M.; Luget, A.; Wilson, R. *Thermochim. Acta* **1994**, 238, 295.
- (11) Hourston, D. J.; Song, M.; Hammiche, A.; Pollock, H. M.; Reading, M. *Polymer* **1997**, 38, 1.
- (12) Schawe, J. E. K. *Thermochim. Acta* **1995**, 261, 183.
- (13) Schawe, J. E. K.; Höhne, G. W. H. *Thermochim. Acta* **1996**, 287, 213.
- (14) Hensel, A.; Dobbertin, J.; Boller, A.; Schawe, J. E. K. *J. Therm. Anal.* **1996**, 46, 935.
- (15) Boller, A.; Schick, C.; Wunderlich, B. *Thermochim. Acta* **1995**, 266, 97.
- (16) Boller, A.; Okazaki, I.; Wunderlich, B. *Thermochim. Acta* **1996**, 284, 1.
- (17) Wunderlich, B.; Boller, A.; Okazaki, I.; Kreitmeier, S. *Thermochim. Acta* **1996**, 282/283, 143.
- (18) Wunderlich, B. *J. Therm. Anal.* **1997**, 48, 207.
- (19) Hutchinson, J. M.; Montserrat, S. *Thermochim. Acta* **1996**, 286, 263.
- (20) Moynihan, C. T.; et al. *Ann. N.Y. Acad. Sci.* **1976**, 279, 15.
- (21) Kovacs, A. J.; Aklonis, J. J.; Hutchinson, J. M.; Ramanos, A. R. *J. Polym. Sci., Polym. Phys. Ed.* **1979**, 17, 1097.
- (22) Narayanaswamy, O. S. *J. Am. Ceram. Soc.* **1971**, 54, 491.
- (23) Hodge, I. M. *Macromolecules* **1987**, 20, 2897.
- (24) Mohanty, U. *Adv. Chem. Phys.* **1995**, 89, 89.
- (25) Hodge, I. M.; Berens, A. R. *Macromolecules* **1981**, 14, 1599.
- (26) Berens, A. R.; Hodge, I. M., *Macromolecules* **1982**, 15, 756.
- (27) Hodge, I. M.; Berens, A. R., *Macromolecules* **1982**, 15, 762.
- (28) Oudhuis, A. A. C. M.; ten Brinke, G. *Macromolecules* **1992**, 25, 698.
- (29) Bosma, M.; ten Brinke, G.; Ellis, T. S. *Macromolecules* **1988**, 21, 1465.
- (30) ten Brinke, G.; Oudhuis, A. A. C. M.; Ellis, T. S. *Thermochim. Acta* **1994**, 238, 75.
- (31) Pappin, A. J.; Hutchinson, J. M.; Ingram, M. D. *Macromolecules* **1992**, 25, 1084.
- (32) Oudhuis, A. A. C. M.; ten Brinke, G.; Karasz, F. E. *Polymer* **1993**, 34, 1991.
- (33) Alberda van Ekenstein, G. O. R.; ten Brinke, G.; Ellis, T. S. In *Glassy Polymers*; ACS Symposium Series; to be published.
- (34) van Assche, G.; van Hemelrijck, A.; Rahier, H.; van Mele, B. *Thermochim. Acta* **1995**, 268, 121.
- (35) van Assche, G.; van Hemelrijck, A.; Rahier, H.; van Mele, B. **1996**, 286, 209.

MA970902T